Received: 16 October 2024 | Revised: 14 November 2024 | Accepted: 18 November 2024

DOI: 10.1002/ardp.202400814

FULL PAPER

ARCH PHARM DPhG
Archiv der Pharmazie

Exploring aliphatic sulfonamides as multiclass inhibitors of the carbonic anhydrases from the pathogen bacterium *Vibrio cholerae*

Niccolò Paoletti[1] | Simone Giovannuzzi[2] | Alessandro Bonardi[1] | Viviana De Luca[3] | Clemente Capasso[3] | Alessio Nocentini[2] | Paola Gratteri[1] | Claudiu T. Supuran[2]

[1]NEUROFARBA Department, Laboratory of Molecular Modelling, Cheminformatics & QSAR, University of Florence, Firenze, Italy

[2]NEUROFARBA Department, Pharmaceutical and Nutraceutical Section, University of Florence, Firenze, Italy

[3]Department of Biology, Agriculture and Food Sciences, National Research Council (CNR), Institute of Biosciences and Bioresources, Naples, Italy

Correspondence
Paola Gratteri, NEUROFARBA Department, Laboratory of Molecular Modelling, Cheminformatics & QSAR, University of Florence, Sesto Fiorentino 50019, Firenze, Italy.
Email: paola.gratteri@unifi.it

Simone Giovannuzzi, NEUROFARBA Department, Pharmaceutical and Nutraceutical Section, University of Florence, Sesto Fiorentino 50019, Firenze, Italy.
Email: simone.giovannuzzi@unifi.it

Funding information
European Union's Horizon 2020 research and innovation programme, Grant/Award Number: 951883

Abstract

This study investigates aliphatic sulfonamide derivatives as inhibitors of the α-, β-, and γ-class carbonic anhydrase (CA) isoforms from *Vibrio cholerae* (VchCAs). A series of 26 compounds bearing a triazole linker and urea- or ether-based tails were described and evaluated for their inhibitory action using a stopped-flow CO_2 hydrase technique. These inhibitors demonstrated a preferential efficacy against VchCAβ. Specifically, the ureido derivatives showed the highest inhibitory potency with inhibition constants (K_Is) in the submicromolar range (0.67–0.93 µM). Selectivity indices were calculated to assess the selective inhibition of VchCAβ over human CA I and II, as well as other VchCA isozymes. Urea-linked compounds demonstrated a significant 25- to 125-fold selectivity for VchCAβ over hCAs and 14- to 26-fold over other VchCAs. Molecular modeling elucidated the interactions contributing to the efficacy and selectivity of aliphatic sulfonamides as VchCA inhibitors, aligning with and reinforcing the experimental results. The latter suggests that aliphatic sulfonamides could serve as valid targeted therapeutics to treat *V. cholerae* infections.

KEYWORDS
aliphatic sulfonamides, bacterial carbonic anhydrase, enzyme inhibition, Gram-negative, *Vibrio cholerae*

1 | INTRODUCTION

Cholera is a highly contagious acute diarrheal disease caused by the Gram-negative bacillus *Vibrio cholerae*.[1] Morbidity and mortality associated with this disease remain significant issues in developing countries. With appropriate treatment, the mortality rate is less than 0.2%; however, without treatment, the mortality rate can be as high as 50%–70%.[1–4] It is estimated that cholera causes between 21,000 and 143,000 deaths worldwide annually.[3] The key symptoms of cholera include profuse watery diarrhea, vomiting, and leg cramps.[2] Cholera treatment involves rapid rehydration through oral or intravenous fluids, which is crucial in managing cholera cases to prevent severe dehydration, electrolyte imbalances, and potentially fatal outcomes. Adjunctive treatment with antibiotics, such as tetracyclines, fluoroquinolones, and macrolides, is beneficial in moderate to severe cases. However, several *V. cholerae* strains are resistant to tetracycline and sometimes to multiple antibiotics.[5–8]

Anyhow, considering that Vibrio spp. are bacteria present in freshwater, estuarine and marine environments, improved sanitation, access to clean water, and public health education could play an essential role in cholera prevention and control strategies in at-risk and developing regions.[2,4]

Up to now, two oral inactivated cholera vaccines are also available: WC/rBS (licensed in the USA) and BivWC (used in endemic areas), which are administered in two or three doses and provide 60%–85% protection for 2–3 years.[9,10] To colonize human hosts, *V. cholerae* secretes virulence factors, the most significant being cholera toxin (CT), which is essential for the manifestation of cholera effects resulting in massive diarrhea.[11,12] In fact, new therapies targeting virulence genes, toxin production, and colonization by *V. cholerae* could be beneficial, especially as alternatives to antibiotics become increasingly necessary.[12–14]

One of the key physiological reactions for the life cycle of most organisms, including bacteria, is the hydration/dehydration of CO_2. This reaction is linked to numerous metabolic pathways, such as those requiring CO_2 or HCO_3^-, and processes including pH homeostasis, electrolyte secretion, and CO_2 and bicarbonate transport.[15,16] The reversible hydration of CO_2 is catalyzed by essential enzymes called carbonic anhydrases (CAs), which are a superfamily of metalloenzymes, preferentially including a Zinc(II) atom. The genome of *Vibrio cholerae* encodes for three CAs including *Vibrio cholerae* carbonic anhydrase (VchCA)α, VchCAβ, and VchCAγ from the α-CA, β-CA, and γ-CA classes, respectively.[17,18] These enzymes play important roles in bacterial cellular metabolism and pH homeostasis and could represent potential targets for developing anti-infective therapies with the aim of preventing *V. cholerae* colonization. The three-dimensional (3D) structure of VchCAβ (PDB 5CXK), solved by X-ray crystallography in 2015 by Supuran and co-workers,[19] revealed a tetrameric type II β-CA. In 2021, the same group proposed models built by homology for VchCAα and VchCAγ.[18]

Searching for new inhibitor chemotypes for the design of CA inhibitors, we developed a series of aliphatic sulfonamide derivatives, which demonstrated very potent inhibitory activity against human CA III, but mild inhibitory effects against a plethora of other human isoforms, among which hCA II, IV, VII, and XII. Therefore, considering the different active site architectures among α-, β-, and γ-CAs, the purpose of our work is to provide new information about the potential of aliphatic sulfonamides as inhibitors of three CA-classes belonging to *Vibrio cholerae*, adopting in silico methodologies to study the structure–activity relationship.

2 | RESULTS AND DISCUSSIONS

Vchα was the first isoform from *V. cholerae* cloned, purified, and characterized in 2012 by Capasso and co-workers. This enzyme showed significant catalytic activity. Moreover, a study with sulfonamides and sulfamates led to the discovery of a variety of low nanomolar inhibitors, including methazolamide (**I**), acetazolamide (AAZ) (**II**), and ethoxzolamide (**III**), with K_I values ranging from 0.69 to 8.1 nM (Figure 1).[20] Subsequently, in 2014, Ceruso et al. and Alafeefy et al. expanded the set of sulfonamide-based inhibitors, discovering nanomolar inhibitors of pathogenic bacteria. Among these, compounds **IV** and **V**, a quinazoline-based inhibitor, exhibited promising potency and selectivity for Vchα over human carbonic anhydrase (hCA) I and II, with K_I values of 8.8 nM (selectivity index [SI] > 550) and 8.5 nM (SI > 25.7), respectively.[21,22]

Vchβ was cloned, purified, and structurally characterized in 2015 by Ferraroni et al.,[19] revealing a tetrameric type II β-CA. AAZ (**II**) was found to be a weak inhibitor of this isozyme, with a K_I in the micromolar range (452 μM). In 2016, Capasso and co-workers improved the series of arylsulfonamide-based inhibitors, confirming the limited inhibitory capacity of the β isozyme.[23] Few months later, the third

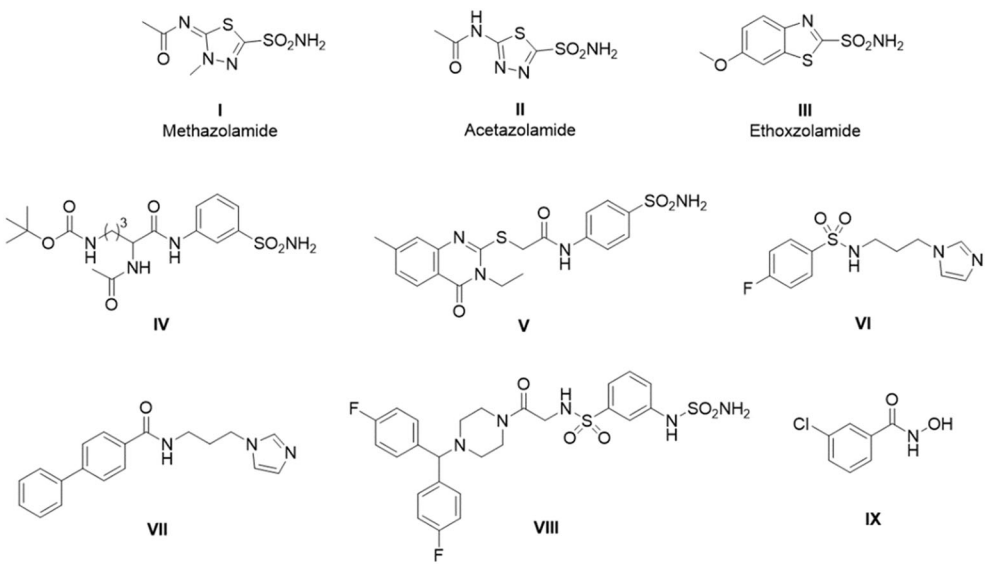

FIGURE 1 Structure of carbonic anhydrase (CA) inhibitors **I**–**IX**.

VchCA, VchCAγ, was discovered and characterized in 2016 by Del Prete et al., confirming its classification in the γ-class. In contrast to the β isoform, VchCAγ was strongly inhibited by sulfonamide-based compounds, such as Ethoxzolamide (**III**), which exhibited a low nanomolar inhibition with a K_I of 85.1 nM.[24] Continued research in subsequent years led to the discovery of new VchCA inhibitors with various CA inhibitory scaffolds. In 2017, Supuran and co-workers tested imidazole-based and secondary sulfonamide-based inhibitors against VchCAα, identifying nanomolar inhibitors such as compounds **VI** and **VII** with K_Is of 8.5 and 5.4 nM, respectively (Figure 1).[25] In the same year, Angeli et al.[26] evaluated acyl selenoureido benzenesulfonamide, showing subnanomolar inhibition for isozyme α and micromolar inhibition for β isoform. A similar trend was observed in 2018 by Bua et al., who introduced a novel series of sulfimide-based compounds as VchCA inhibitors, favoring nanomolar inhibition against VchCAα and micromolar inhibition against VchCAβ, as demonstrated by derivative **VIII** (VchCAα: K_I = 91.4 nM, VchCAβ: K_I > 10000 nM) (Figure 1).[27] Another CA inhibitor chemotype was also evaluated in 2018 by Berrino et al., which provided a kinetic study against all VchCA with a panel of N'-aryl-N-hydroxy-ureas.[28] This set of peculiar inhibitors showed a better inhibition against the VchCAβ isozyme with respect to the α and γ isoforms, for example, compound **IX** (VchCAα: K_I = 4000 nM, VchCAβ: K_I > 60.3 nM, VchCAγ: K_I > 10000 nM) (Figure 1).[28] In 2019, Angeli et al. assessed famotidine, an antiulcer drug belonging to the H2-antagonists class of pharmacological agents, against three VchCAs. Following the behavior of several sulfonamide-based inhibitors, it resulted to be a nanomolar modulator of VchCAα, K_I of 72.3 nM, and a micromolar inhibitor of VchCAβ, K_I of 83917 nM, and VchCAγ, K_I of 5321 nM.[29]

It should be stressed that, since their discovery, VchCAs have been extensively examined for their modulation to offer new perspectives in the CA domain. In fact, alongside the previously discussed inhibitors **I**–**IX** (Figure 1), additional CA modulators have recently emerged as promising regulators of *V. cholerae*. These include benzoxaboroles,[30] poly(amidoamine) derivatives,[31] phenols,[32] coumarins (only against VchCAα, the singular VchCA with hydrolyzing activity),[33] and hydrazones.[34] In this work, we provide fresh insights into the neglected aliphatic sulfonamides, to overcome the selectivity profile of the parent arylsulfonamide derivatives in VChCA inhibition.

The development of aliphatic sulfonamides was facilitated by a scaffold resizing approach (Figure 2). This method was initially employed in 2023 to uncover potent and selective hCA III inhibitors.[35]

Briefly, the synthesis initially involved the incorporation of azide and sulfonic acid moieties by the cleavage of 5- and 6-membered sultones with sodium azide (NaN_3). These formed sulfonic acid moieties, which were converted into the corresponding sulfonyl chlorides using a suitable chlorinating agent, and subsequently transformed into sulfonamides with an ammonia solution. For building the counterpart of the products, several alkyne-based intermediates were synthesized starting from substituted phenols or isocyanates which were respectively reacted with propargyl bromide and propargyl amine under mild conditions. After that, the Cu-catalyzed Huisgen-cycloaddition reaction was applied to form the triazole as a linker between aliphatic sulfonamides and different tails, achieving compounds **1**–**26**.[35]

2.1 | CA inhibition studies

The CA inhibition profile of compounds **1**–**26** was thus evaluated against three VchCA isoforms by a stopped-flow CO_2 hydrase assay,[36] using AAZ as a reference inhibitor (Table 1). The data against physiologically relevant hCA I and II, as well as SAR discussion, were already reported.[35]

The following structure–activity relationship (SAR) can be gathered from the inhibition data reported in Table 1.

VchCAα is minimally affected by all derivatives **1**–**26**, with K_I values falling within the medium micromolar range. Particularly, K_I values range from 8.43 µM up to 34.4 µM. Notably, compound **8** (*n* = 1), featuring a urea-based link, emerged as the most potent compound with a K_I of 8.43 µM, surpassing its counterpart **21** (*n* = 2) by at least twofold in efficacy. This pattern persisted with other congeners like **5**–**7** and **10**, which exhibited greater potency than **18**–**20** and **23**, respectively. On the other hand, the 3-methoxyphenylureido derivative **22**, with a K_I of 14.0 µM, was the sole compound in this selection to demonstrate more effective inhibition of VchCAα than its lower analog **9**, with a K_I of 17.5 µM. The substitution on the phenyl had a marginal impact on the potency of these compounds. For instance, compounds **5**–**7** displayed K_Is between 11.2 and 13.4 µM, while

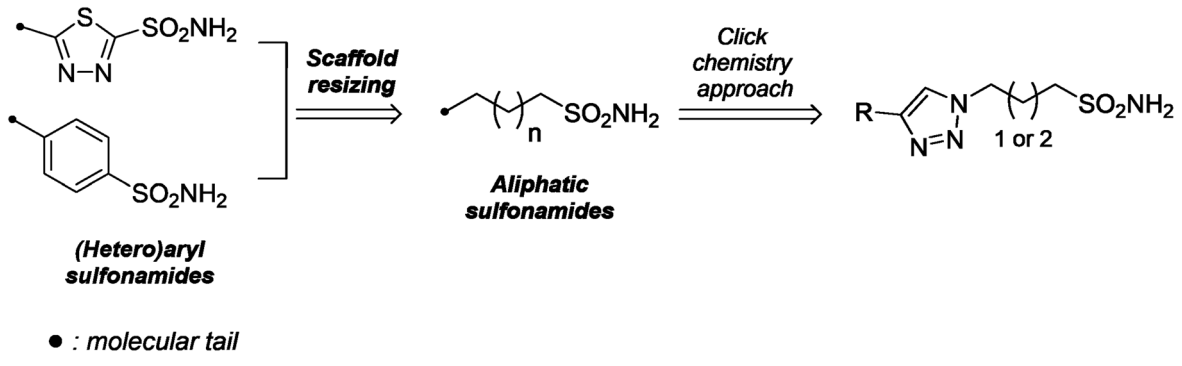

FIGURE 2 The adopted strategy for the synthesis of aliphatic sulfonamide-based derivatives.

TABLE 1 Inhibition activity of derivatives **1–26** and the standard CA inhibitor Acetazolamide (AAZ) against human isoforms hCA I and II and bacterial CAs VchCAα, VchCAβ and VchCAγ belonging to *Vibrio cholerae* by the CO_2 hydrase stopped-flowAssay.

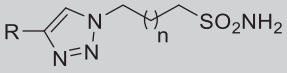

1-26

			K_I (μM)[a]				
			hCA		VchCA		
Code	R	n	I	II	α	β	γ
1	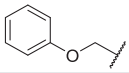	1	0.75	2.72	29.1	4.16	37.8
2	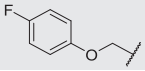	1	4.89	2.02	21.3	3.74	33.1
3	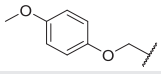	1	1.16	2.44	16.5	2.96	25.6
4	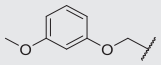	1	1.91	4.10	14.9	3.38	23.8
5	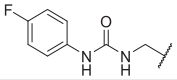	1	>100	2.89	13.4	0.93	12.6
6	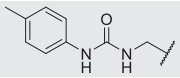	1	>100	2.96	14.6	0.82	10.9
7	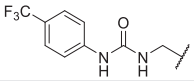	1	>100	4.16	11.2	0.67	17.3
8	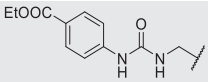	1	>100	2.50	8.43	2.59	15.1
9	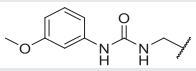	1	>100	0.93	17.5	1.72	9.4
10	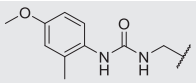	1	>100	0.87	10.6	4.03	11.5
11		1	0.62	0.65	22.6	7.44	53.0
12	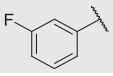	1	0.60	0.71	24.5	7.18	49.3
13	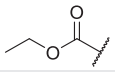	1	0.86	3.14	30.7	9.67	41.9
14	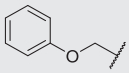	2	6.53	7.76	34.4	6.91	43.5
15	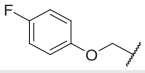	2	6.42	8.12	25.1	5.89	39.7
16	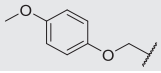	2	8.54	3.93	28.7	6.13	40.3
17	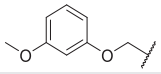	2	2.31	5.97	26.6	4.97	36.1
18	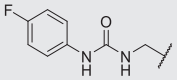	2	5.38	7.57	16.9	3.41	20.6
19	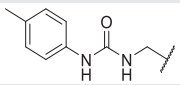	2	5.29	4.93	18.3	2.86	15.3
20	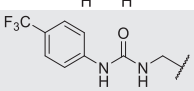	2	5.38	0.78	16.8	3.00	16.8

TABLE 1 (Continued)

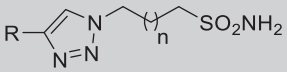

1-26

			K_I (μM)[a]				
			hCA		VchCA		
Code	R	n	I	II	α	β	γ
21	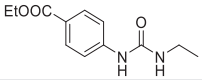	2	6.52	0.56	20.4	5.08	18.4
22	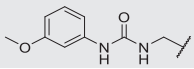	2	5.51	4.60	14.0	1.97	22.2
23	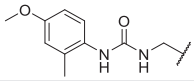	2	>100	8.15	12.6	2.14	14.6
24		2	0.91	0.77	27.8	8.35	62.3
25	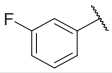	2	3.27	0.80	31.4	8.04	60.6
26	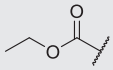	2	0.77	8.13	30.1	11.3	75.0
AAZ	-	-	0.25	0.012	0.0068	0.452	0.473

Abbreviations: AAZ, acetazolamide; hCA, human carbonic anhydrase; VchCA, *Vibrio cholerae* carbonic anhydrase.

[a]Mean from three different assays, by a Stopped-Flow technique (errors were in the range of ±5%–10% of the reported values).

18–**20** showed K_Is between 16.8 and 18.3 μM. The ether-based link derivatives **1**–**4** were detected as poor inhibitors of this isoform, exhibiting K_Is of 14.9–29.1 μM. In particular, the presence of a methoxy group on the phenyl moiety improves the potency, as seen with compounds **3** and **4** with K_Is of 16.5 and 14.9 μM, respectively, while the superior analogs **16** and **17** exhibited a lower activity, with K_Is of 28.7 and 26.6 μM, but comparable to that of their congener **15**, K_I of 25.1 μM, featuring a fluorine atom as a substituent. Compounds with nonsubstituted phenyl moiety, such as **1**, K_I of 29.1 μM, and **14,** K_I of 34.4 μM, demonstrated a diminished potency, with **14** being the least effective inhibitor against this isoform. Finally, compounds **11**–**13** and **24**–**26** exhibited comparable activity against VchCAα ranging from 22.6 to 31.4 μM. Compound **11**, K_I of 22.6 μM, demonstrated a more potent inhibition than the superior analog **24**, K_I of 27.8 μM, as well as **12** and **25**, with K_Is of 24.5 and 31.4 μM, respectively. On the other side, the length of the chain did not significantly affect the K_Is of **13** and **26**, which were 30.7 and 30.1 μM, respectively.

VchCAβ is the most inhibited isoform by the CA inhibitors studied **1**–**26**, with K_I values ranging from high nanomolar to medium micromolar, specifically between 0.67 and 11.3 μM. The urea-based compounds were the most effective inhibitors, exhibiting K_Is even in the nanomolar range. In fact, the most potent inhibitor identified is derivative **7**, with a K_I of 0.67 μM. Compounds **5** and **6** also showed impressive inhibition profiles, with K_I values of 0.93 and 0.82 μM, respectively. All these compounds feature a para-substituted phenyl with lipophilic substituents such as fluorine (**5**), methyl (**6**), or trifluoromethyl (**7**). However, this promising activity was not observed in their superior analogs **18**–**20**, which exhibited K_I values in the low micromolar range, 3.41, 2.86, and 5.08 μM, respectively. The inhibitory potential of ureidic derivatives was generally influenced by the length of the aliphatic linker, except for the analogs **9**, K_I of 1.72 μM, and **22**, K_I of 1.97 μM. The ether-based linked derivatives also showed variable inhibition, particularly for the *p*-methoxyphenyl substituted compounds **3** ($n = 1$) and **16** ($n = 2$), with K_Is of 2.96 and 6.13 μM, respectively. The methoxy substituent's position did not significantly affect the inhibitory potency of compounds **4** ($n = 1$), K_I of 3.38 μM, and **17** ($n = 2$), K_I of 4.97 μM. Moreover, the absence of substituents on the phenyl produced poor inhibitors of this isoform, **1**, K_I of 4.16 μM, and **14**, K_I of 6.91 μM. Finally, compounds **11**–**13** and **24**–**26**, lacking a specific linker between the CAI chemotype and tail, were the least effective inhibitors, with K_Is ranging from 7.18 to 11.3 μM. It should be noted that the absence of phenyl significantly decreased the potential inhibitory activity of this series, as demonstrated by inhibitors **13** ($n = 1$), K_I of 9.67 μM, and **26** ($n = 2$), K_I of 11.3 μM.

The third and final assessed isoform is VchCAγ, which is the least inhibited by aliphatic sulfonamides **1**–**26**, with K_I values ranging from 9.4 to 75 μM. Compound **9** ($n = 1$), bearing a 3-methoxypheylureidic tail, is the most potent inhibitor of this class showcasing a K_I value in the low micromolar range, 9.4 μM; meanwhile, other derivatives pointed out K_Is in the medium micromolar range. For instance, compounds **5**–**8** and **10** ($n = 1$) are among the poorest inhibitors, with K_I values ranging from 10.9 to 17.3 μM. In comparison with their superior homologs, **18**–**23** ($n = 2$), showing K_Is between 14.6 and

22.2 μM, a shift in the inhibitory activity was observed. In fact, within this subset, compound **23** is the most effective with a K_I of 14.6 μM, while compound **22** is the least potent, with a K_I of 22.2 μM. The ether-based derivatives exhibited a lower inhibitory activity against this isoform, confirming the pattern observed for the previous bacterial α- and β-CAs. In fact, The K_I values for compounds **1**–**4** (n = 1) range from 23.8 to 37.8 μM, while their superior homologs **14**–**17** (n = 2) range from 36.1 to 43.5 μM. Particularly, the presence of a substituted phenyl in the tail part increased the activity of each derivative compared with the nonsubstituted ones, as demonstrated by compounds **2**–**4** (K_Is of 23.8–33.1 μM) over derivative **1** (K_I of 37.8 μM) and compounds **15**–**17** (K_Is of 36.1–40.3 μM) over derivative **14** (K_I of 43.5 μM). Finally, compounds **11**–**13** and **24**–**26** resulted to be the poorest inhibitors of this isoform, with K_I values spanning toward the high part of the medium micromolar range, 41.9–75.0 μM.

Considering that VchCAβ was identified as the most inhibited isozyme among the three classes of CAs in *V. cholerae*, we further present the SI for human CAs I and II, as well as for *V. cholerae* α and γ isozymes, relative to VchCAβ. This analysis aims to clarify the preferential inhibition of these compounds and highlight their selectivity for VchCAβ over both the human isoforms and the other bacterial isozymes.

Regarding the target/off-target CA selectivity ratios of these aliphatic sulfonamides, several compounds exhibited notable I/VchCAβ and II/VchCAβ SIs, ranging from 0.083 to 149.2 and 0.087 to 6.20, respectively (Table 2). Additionally, to demonstrate the preferential inhibition of VchCAβ, the VchCAα/VchCAβ and VchCAγ/VchCAβ selectivity ratios were calculated, with ranges of 2.63–17.8 and 2.85–25.8, respectively. Generally, a random specificity based on the type of linker was observed for human CAs I and II against VchCAβ, while a marked preference for VchCAβ over the α and γ isozymes was noted. Specifically, a similar pattern among the SI values can be observed based on the type of linker and tail. Urea-linked derivatives strongly preferred VchCAβ over other VchCAs and human CAs. Notably, derivatives **5**–**10** and **23** showed superior SI values for hCA I/VchCAβ (Table 2), reaching at least two orders of magnitude selectivity, with SI values ranging from 24.8 to 149.2. Furthermore, some compounds also demonstrated significant selectivity for VchCAβ against the α and γ isoforms. For example, compounds **5**–**7** maintained one order of magnitude selectivity for the β-class over the α (SI: 14.4–17.8) and γ (SI: 13.2–25.8) isoforms. In contrast, the ether-based linked derivatives did not show preferential inhibition for VchCAβ, as indicated by their SI values for hCA I/VchCAβ and hCA II/VchCAβ, with most SI values being less than 1. Specifically, compounds **1** (SI: hCA I/VchCAβ, 0.18), **3** (SI: hCA I/VchCAβ, 0.39), **4** (SI: hCA I/VchCAβ, 0.56), and **17** (SI: hCA I/VchCAβ, 0.46) showed good selectivity for hCA I, which then decreased for hCA II, indicating comparable inhibition to that against VchCAβ. Considering the three VchCAs, compounds **1**–**4** and **14**–**17** exhibited low selectivity for the β-class, with SI values ranging from 4.26 to 6.99 (VchCAα/VchCAβ) and 6.29 to 9.08 (VchCAγ/VchCAβ). Finally, compounds **11**–**13** and **24**–**26** exhibited strong selectivity for the human CAs over VchCAβ, with some being up to 100-fold more selective. This is demonstrated by compounds **11**–**13** (SI: hCA I/VchCAβ, 0.083–0.088) and **26** (SI: hCA I/VchCAβ, 0.068) for hCA I, and compounds **11** (SI: hCA II/VchCAβ, 0.087), **12** (SI: hCA II/VchCAβ, 0.099), **24** (SI: hCA II/VchCAβ, 0.092), and **25** (SI: hCA II/VchCAβ, 0.099) for hCA II. Among the VchCAs, these compounds showed low selectivity for the β-class over the α and γ types, with SI values greater than **1**.

TABLE 2 The selectivity index (SI) of derivatives **1**–**26** has been assessed between human CAs I and II against VchCAβ, as well as between VchCAα and VchCAγ against VchCAβ.

	Selectivity index (SI)			
Code	hCA I/ VchCAβ	hCA II/ VchCAβ	VchCAα/ VchCAβ	VchCAγ/ VchCAβ
1	0.18	0.65	6.99	9.08
2	1.30	0.54	5.69	8.85
3	0.39	0.82	5.57	8.64
4	0.56	1.21	4.40	7.04
5	>107.5	3.10	14.4	13.5
6	>121.9	3.60	17.8	13.2
7	>149.2	6.20	16.7	25.8
8	>38.6	0.96	3.25	5.83
9	>58.3	0.54	10.1	5.46
10	>24.8	0.21	2.63	2.85
11	0.083	0.087	3.03	7.12
12	0.084	0.099	3.41	6.86
13	0.088	0.32	3.17	4.33
14	0.94	1.12	4.97	6.29
15	1.08	1.37	4.26	6.74
16	1.39	0.64	4.68	6.57
17	0.46	1.20	5.35	7.26
18	1.57	2.21	4.95	6.04
19	1.84	1.72	6.39	5.34
20	1.79	0.26	5.6	5.60
21	1.28	0.11	4.01	3.62
22	2.79	2.33	7.10	11.2
23	>46.7	3.80	5.88	6.82
24	0.11	0.092	3.32	7.46
25	0.40	0.099	3.90	7.53
26	0.068	0.72	2.66	6.63
AAZ	0.55	0.026	0.015	1.04

Abbreviations: AAZ, acetazolamide; hCA, human carbonic anhydrase; VchCA, *Vibrio cholerae* carbonic anhydrase.

2.2 | In silico studies

In silico studies were performed to clarify the binding mode of aliphatic sulfonamides within the active sites of VchCAs. Currently, no solved crystal structures are available in the Protein Data Bank (PDB)[37] for VchCAα, VchCAγ, and type I/open VchCAβ. Therefore, docking simulations were carried out using homology-built models of the three *Vibrio cholerae* CAs, according to the previously reported procedures.[30] To assess the impact of the linker type and aromatic tail substitution on the ligand-target interaction, compounds **2**, **7**, and **12** were selected as representative ligands for this study. According to the literature,[18] all docking solutions found the deprotonated nitrogen atom of the sulfonamide group (SO_2NH^-) bound to the zinc ion, completing the tetragonal coordination geometry of the metal in all three VchCAs.

In the VchCAα active site, two H-bonds are formed between the zinc-bound sulfonamide NH^- and S=O groups with the side chain OH and the backbone NH of T199, respectively, which further stabilizes the ligands within the active site (Figure 3a–c). The aliphatic linker between the sulfonamide group and the triazole is centrally located within the cavity, allowing the five-membered cycle to form van der Waals (vdW) interactions solely with the L188 residue. The aromatic tail of compound **2** forms a π–π stacking interaction with the indole of W23 (Figure 3a). However, the shorter tail of compound **12**,

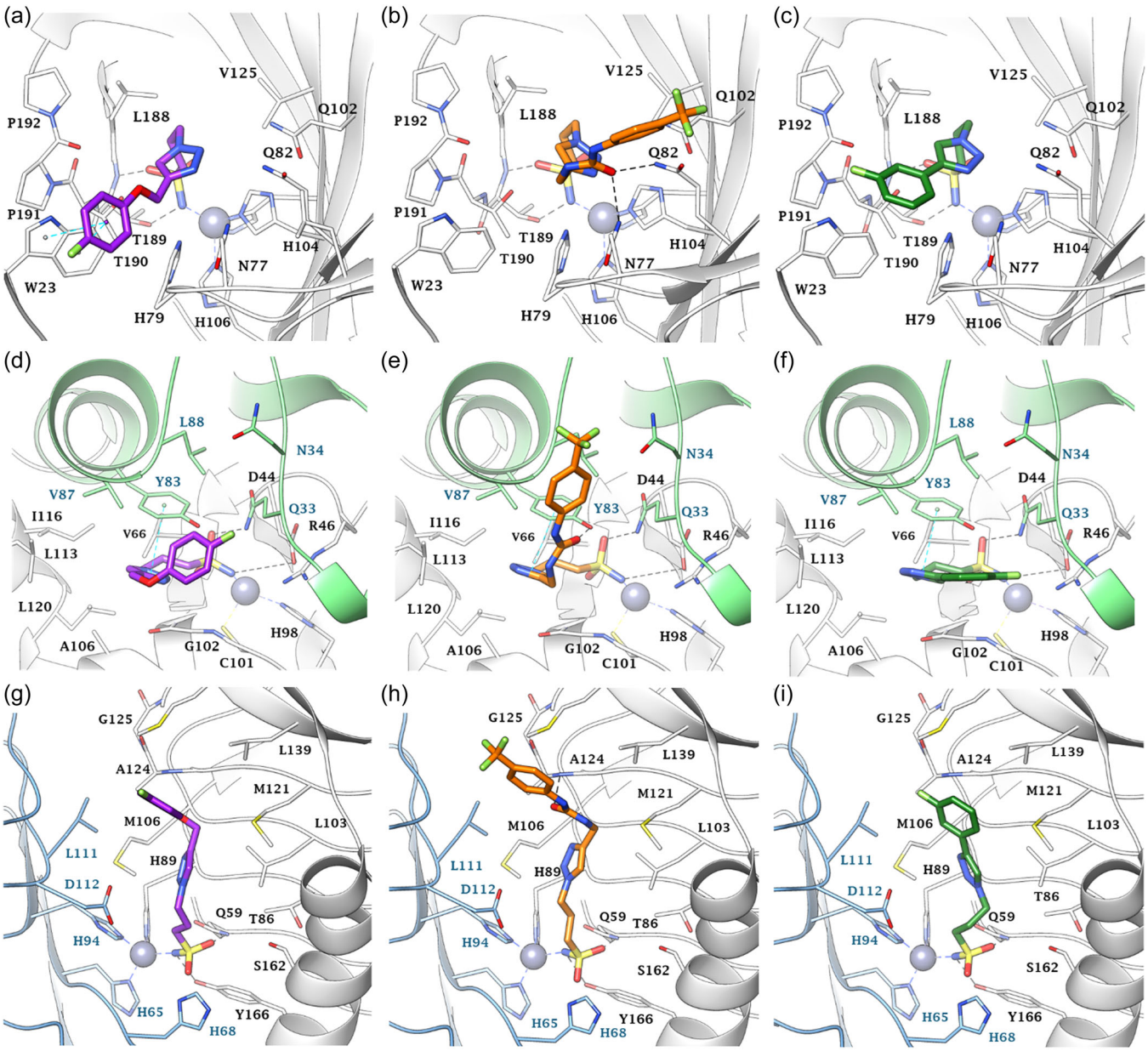

FIGURE 3 Predicted binding mode of compounds **2** (purple), **7** (orange), and **12** (green) within VchCAα (a–c), VchCAβ (d–f), and VchCAγ (g–i) active sites. H-bonds and π–π stacking interactions are depicted as black and cyan dashed lines, respectively. Amino acid labels are colored according to the a (black) and b (blue) chains (d–i). VchCAs, *Vibrio cholerae* carbonic anhydrase.

compared with ligand **2**, prevents the formation of such an interaction (Figure 3c). In contrast, the urea linker in compound **7** forms two H-bonds between its C=O group and the NH_2 side chains of N77 and Q82, causing the aromatic tail to be located in a different pocket of the active site (Figure 3b).

In the dimeric and narrow VchCAβ-binding pocket, the sulfonamide zinc-binding motif of the ligands participates in two H-bonds with the residues D44 (chain A) and Q33' (chain B), reinforcing the stability of the complex. The aliphatic chain is involved in several vdW contacts with V66, Y83', and G102, and in addition, the triazole is stacked with the phenolic side chain of Y83', which is typically involved in the stabilization of aromatic sulfonamides, forming π–π interactions (Figure 3d,e). In compound **7**, the carbonyl group of the urea linker is in H-bond distance to the Y83' side chain, contributing to the stability of the binding pose and also orienting the aromatic tail differently within the binding site (Figure 3e).

Within the dimeric VchCAγ active site, the coordination of the ligand to the zinc ion is further stabilized by two H-bonds between the sulfonamide group and the side chain NH_2 and OH of Q59 and Y166, respectively (Figure 3g–i). However, the docking solutions predict a linear arrangement of the three compounds at the center of the cylindrical VchCAγ active site, which limits both polar interactions and hydrophobic contacts. In this arrangement, the carbonyl C=O in the urea linker of compound **7** forms an H-bond with the backbone NH of A124 (Figure 3h).

Overall, the greater inhibitory ability of compound **7** compared with compounds **2** and **12**, observed across the three isoforms (Table 1), may be related to the urea linker's ability to engage in polar interactions. Additionally, the enhanced inhibition of all three ligands toward VchCAβ, as opposed to VchCAα and VchCAγ, can be explained by the smaller size of the VchCAβ active site, particularly near the catalytic zinc ion, which allows for maximized hydrophobic contacts with the ligands' aliphatic linker.

3 | CONCLUSION

This study presents a series of aliphatic sulfonamide derivatives acting as potential inhibitors of the *V. Cholerae*-expressed CAs, α-, β- and γ-VchCA. The design of these inhibitors, featuring a triazole linker and urea- or ether-based tails, exhibited a preferential inhibition of the VchCAβ over the VchCAα and VchCAγ, pointing out K_I values ranging from high nanomolar to medium micromolar concentrations. Among them, the urea-based derivatives **5**–**10** and **18**–**23** stood out as the most potent subset demonstrating a superior inhibitory activity. The SIs emphasized such preferential inhibition toward the VchCAβ over the other two microbial isozymes and also over the human isoforms I and II, which are considered the main off-targets. The predicted in silico analyses on compounds **2**, **7**, and **12** provided a deeper understanding of the molecular interactions that explain this selectivity, further reinforcing the experimental observations. In fact, such predictions suggested that compounds belonging to the urea-based subsets, **5**–**10** and **18**–**23**, form more extensive interactions within the active site of the VchCAβ, which may explain their major inhibitory efficacy. Overall, the findings present a novel intriguing chemotype for the inhibition of CAs expressed by *V. cholerae* with a primary specificity for the β isozyme over the α and γ isozymes. Accordingly, this could pave the way for the selective inhibition of a specific family of CAs, thereby reducing the risk of side effects and unwanted consequences associated with pan-CA inhibition.

4 | MATERIALS AND METHODS

4.1 | Chemistry

Synthetic procedures and compound characterization are reported in Giovannuzzi et al.[35]

4.2 | CA inhibition

The CA-catalyzed CO_2 hydration activity has been measured with an Applied Photophysics stopped-flow instrument.[36] The used pH indicator was phenol red (at a concentration of 0.2 mM), working at the absorbance maximum of 557 nm. A volume of 10 mM HEPES (pH 7.4) was employed as a buffer, in the presence of 10 mM $NaClO_4$ to maintain the ionic strength constant. The initial rates of the CA-catalyzed CO_2 hydration reaction were followed up for a period of 10–100 s. The substrate CO_2 concentrations ranged from 1.7 to 17 mM for determining the inhibition constants. For each inhibitor, at least six traces of the initial 5%–10% of the reaction were used to determine the initial velocity. The uncatalyzed rates were determined in the same manner and subtracted from the total observed rates. Stock solutions of inhibitors (10 mM) were prepared in distilled-deionized water with a maximum of 5% DMSO, and dilutions up to 10 nM were done thereafter with the assay buffer. Inhibitor and enzyme solutions were preincubated together for 1–6 h before the assay, to allow for the formation of the enzyme-inhibitor complex. The inhibition constants were obtained by nonlinear least-squares methods using Prism 3 and the Cheng-Prusoff equation, as reported previously, and represent the mean from at least three different determinations. All enzymes employed were recombinant and obtained in-house as reported,[35] with concentrations in the assay ranging from 5 to 12 nM. The human/protozoan enzymes were recombinant proteins obtained in-house, as described earlier.[30,32]

4.3 | In silico studies

The experimental protocol used for the development of the VchCAα, VchCAβ, and VchCAγ homology models was described in Bonardi et al.[30] The primary sequences of VchCAα and VchCAγ were retrieved from the UniProt Consortium. The crystal structure of α-CA from Photobacterium profundum (PDB 5HPJ)[38] and γ-CA homologous

protein from *Escherichia coli* (PDB 3TIO)[39] were used as templates in the homology modeling procedure. Multiple models were generated using the Prime module of Schrödinger[40a] and the SwissModel platform (https://swissmodel.expasy.org/) and submitted to loop refinement and quality evaluation procedures (Supporting Information S1: Figures S1–S9 and Tables S1–S3).[30] The best-scored structures of VchCAα and VchCAγ and the VchCAβ crystal structure (retrieved as PDB 5CXK)[19] were prepared for docking using the Protein Preparation Wizard tool, using the OPLS4 force field[41–43] and applying an energy minimization protocol with a root mean square deviation (RMSD) value of 0.30 Å. Ligand structures were generated using Maestro[40b] and their ionization states were evaluated at pH 7.4 ± 0.5 using Epik.[40c] Energy minimization of the ligands was carried out using the conjugate gradient method in Macromodel,[40e] with a maximum of 2500 iterations and a convergence criterion of 0.05 kcal mol^{-1} $Å^{-1}$. Docking was performed with Glide,[40f] centering grids on the centroids of the zinc-coordinating residues, and ligands were docked using the standard precision (SP) mode. Figures were generated with Maestro and Chimera.[40,44]

ACKNOWLEDGMENTS

This research was funded by the European Union's Horizon 2020 research and innovation programme under grant agreement No. 951883 within the SPRINGBOARD project (to CT Supuran). Open access publishing facilitated by Universita degli Studi di Firenze, as part of the Wiley - CRUI-CARE agreement.

CONFLICTS OF INTEREST STATEMENT

The authors declare no conflicts of interest.

DATA AVAILABILITY STATEMENT

The data that support the findings of this study are available from the corresponding author upon reasonable request.

ORCID

Niccolò Paoletti http://orcid.org/0000-0002-6874-9419
Simone Giovannuzzi http://orcid.org/0000-0002-0669-7481
Alessandro Bonardi http://orcid.org/0000-0002-5520-740X

REFERENCES

[1] D. A. Montero, R. M. Vidal, J. Velasco, S. George, Y. Lucero, L. A. Gómez, L. J. Carreño, R. García-Betancourt, M. O'Ryan, *Front. Med.* **2023**, *10*, 1155751.
[2] M. W. LeChevallier, T. Prosser, M. Stevens, *Microorganisms* **2024**, *12*, 916.
[3] F. K. Agyei, B. Scharf, S. Duodu, *Trop. Med. Infect. Dis.* **2024**, *9*, 103.
[4] L. D'Mello-Guyett, K. Gallandat, R. Van den Bergh, D. Taylor, G. Bulit, D. Legros, P. Maes, F. Checchi, O. Cumming, *PLoS One* **2020**, *15*, e0226549.
[5] B. Das, J. Verma, P. Kumar, A. Ghosh, T. Ramamurthy, *Vaccine* **2020**, *38*(Suppl 1), A83.
[6] N. Rivard, R. R. Colwell, V. Burrus, *mSphere* **2020**, *5*, e00748-20.
[7] M. H. Ahmadi, *Antimicrob. Resist. Infect. Control* **2021**, *10*, 115.
[8] B. E. Igere, H. Onohuean, D. C. Iwu, E. O. Igbinosa, *Infect. Med.* **2023**, *2*, 283.
[9] M. M. Levine, F. Noriega, *Papua New Guinea Med. J.* **1995**, *38*, 325.
[10] J. Holmgren, A. M. Svennerholm, *Scand. J. Infect. Dis. Suppl.* **1990**, *70*, 149.
[11] D. Vanden Broeck, C. Horvath, M. J. S. De Wolf, *Int. J. Biochem. Cell. Biol.* **2007**, *39*, 1771.
[12] C. Muanprasat, V. Chatsudthipong, *Future Med. Chem.* **2013**, *5*, 781.
[13] M. S. Zahid, S. P. Awasthi, M. Asakura, S. Chatterjee, A. Hinenoya, S. M. Faruque, S. Yamasaki, *PLoS One* **2015**, *10*, e0137529.
[14] M. S. H. Zahid, S. P. Awasthi, A. Hinenoya, S. Yamasaki, *J. Vet. Med. Sci.* **2015**, *77*, 535.
[15] C. T. Supuran, C. Capasso, *Metabolites* **2017**, *7*, 56.
[16] C. T. Supuran, *Front. Pharmacol.* **2011**, *2*, 34.
[17] F. Mancuso, L. De Luca, F. Bucolo, M. Vrabel, A. Angeli, C. Capasso, C. T. Supuran, R. Gitto, *Chem. Med. Chem.* **2021**, *16*, 3787.
[18] A. Bonardi, A. Nocentini, S. M. Osman, F. A. Alasmary, T. M. Almutairi, D. S. Abdullah, P. Gratteri, C. T. Supuran, *J. Enzyme Inhib. Med. Chem.* **2021**, *36*, 469.
[19] M. Ferraroni, S. Del Prete, D. Vullo, C. Capasso, C. T. Supuran, *Acta Crystallogr. D. Biol. Crystallogr.* **2015**, *71*, 2449.
[20] S. Del Prete, S. Isik, D. Vullo, V. De Luca, V. Carginale, A. Scozzafava, C. T. Supuran, C. Capasso, *J. Med. Chem.* **2012**, *55*, 10742.
[21] M. Ceruso, S. Del Prete, Z. Alothman, C. Capasso, C. T. Supuran, *ACS Med. Chem. Lett.* **2014**, *5*, 826.
[22] A. M. Alafeefy, M. Ceruso, A. M. S. Al-Tamimi, S. Del Prete, C. Capasso, C. T. Supuran, *Bioorg. Med. Chem.* **2014**, *22*, 5133.
[23] S. Del Prete, D. Vullo, V. De Luca, V. Carginale, M. Ferraroni, S. M. Osman, Z. AlOthman, C. T. Supuran, C. Capasso, *Bioorg. Med. Chem.* **2016**, *24*, 1115.
[24] S. Del Prete, D. Vullo, V. De Luca, V. Carginale, S. M. Osman, Z. AlOthman, C. T. Supuran, C. Capasso, *Bioorg. Med. Chem. Lett.* **2016**, *26*, 1941.
[25] D. De Vita, A. Angeli, F. Pandolfi, M. Bortolami, R. Costi, R. Di Santo, E. Suffredini, M. Ceruso, S. Del Prete, C. Capasso, L. Scipione, C. T. Supuran, *J. Enzyme Inhib. Med. Chem.* **2017**, *32*, 798.
[26] A. Angeli, G. Abbas, S. Del Prete, F. Carta, C. Capasso, C. T. Supuran, *Bioorg. Chem.* **2017**, *75*, 170.
[27] S. Bua, E. Berrino, S. Del Prete, V. S. Murthy, V. Vijayakumar, Y. Tamboli, C. Capasso, E. Cerbai, A. Mugelli, F. Carta, C. T. Supuran, *J. Enzyme Inhib. Med. Chem.* **2018**, *33*, 1125.
[28] E. Berrino, M. Bozdag, S. Del Prete, F. A. S. Alasmary, L. S. Alqahtani, Z. AlOthman, C. Capasso, C. T. Supuran, *J. Enzyme Inhib. Med. Chem.* **2018**, *33*, 1194.
[29] A. Angeli, M. Pinteala, S. S. Maier, S. Del Prete, C. Capasso, B. C. Simionescu, C. T. Supuran, *J. Enzyme Inhib. Med. Chem.* **2019**, *34*, 644.
[30] A. Bonardi, A. Nocentini, R. Cadoni, S. Del Prete, P. Dumy, C. Capasso, P. Gratteri, C. T. Supuran, J. Y. Winum, *ACS Med. Chem. Lett.* **2020**, *11*, 2277.
[31] F. Carta, S. M. Osman, D. Vullo, Z. AlOthman, S. Del Prete, C. Capasso, C. T. Supuran, *Bioorg. Med. Chem.* **2015**, *23*, 6794.
[32] S. Giovannuzzi, C. S. Hewitt, A. Nocentini, C. Capasso, G. Costantino, D. P. Flaherty, C. T. Supuran, *J. Enzyme Inhib. Med. Chem.* **2022**, *37*, 666.
[33] S. Giovannuzzi, C. S. Hewitt, A. Nocentini, C. Capasso, D. P. Flaherty, C. T. Supuran, *J. Enzyme Inhib. Med. Chem.* **2022**, *37*, 333.
[34] K. Demir-Yazıcı, Ö. Güzel-Akdemir, A. Angeli, C. T. Supuran, A. Akdemir, *Int. J. Mol. Sci.* **2020**, *21*, 3131.
[35] S. Giovannuzzi, A. Bonardi, P. Gratteri, A. Nocentini, C. T. Supuran, *J. Enzyme Inhib. Med. Chem.* **2023**, *38*, 2202360.
[36] R. G. Khalifah, *J. Biol. Chem.* **1971**, *246*, 2561.
[37] H. M. Berman, *Nucleic Acids Res.* **2000**, *28*, 235.
[38] V. Somalinga, G. Buhrman, A. Arun, R. B. Rose, A. M. Grunden, *PLoS One* **2016**, *11*, e0168022.
[39] H. M. Park, J. H. Park, J. W. Choi, J. Lee, B. Y. Kim, C. H. Jung, J. S. Kim, *Acta Crystallogr. D. Biol. Crystallogr.* **2012**, *68*, 920.

[40] Schrödinger Suite Release **2022**-, 4 Schrödinger, LLC, New York, NY, 2022: (a) Prime, v.5.5; (b) Maestro v.13.2; (c) Epik, v.6.0; (d) Impact, v.9.5; (e) Macromodel v.13.6; (f) Glide, v.9.5.
[41] C. Lu, C. Wu, D. Ghoreishi, W. Chen, L. Wang, W. Damm, G. A. Ross, M. K. Dahlgren, E. Russell, C. D. Von Bargen, R. Abel, R. A. Friesner, E. D. Harder, *J. Chem. Theory Comput*. **2021**, *17*, 4291.
[42] G. A. Kaminski, R. A. Friesner, J. Tirado-Rives, W. L. Jorgensen, *J. Phys. Chem. B* **2001**, *105*, 6474.
[43] M. Abdoli, A. Bonardi, N. Paoletti, A. Aspatwar, S. Parkkila, P. Gratteri, C. T. Supuran, R. Žalubovskis, *Molecules* **2023**, *28*, 4020.
[44] E. F. Pettersen, T. D. Goddard, C. C. Huang, G. S. Couch, D. M. Greenblatt, E. C. Meng, T. E. Ferrin, *J. Comput. Chem.* **2004**, *25*, 1605.

SUPPORTING INFORMATION

Additional supporting information can be found online in the Supporting Information section at the end of this article.

How to cite this article: N. Paoletti, S. Giovannuzzi, A. Bonardi, V. De Luca, C. Capasso, A. Nocentini, P. Gratteri, C. T. Supuran, *Arch. Pharm.* **2025**, *358*, e2400814. https://doi.org/10.1002/ardp.202400814